Sulfur and carbon co-doped g-C_3N_4 microtubes with enhanced photocatalytic H_2 production activity

Yang Ge,[a] Quanhao Shen,[a] Qi Zhang,[a] Naixu Li,[a*] Danchen Lu,[a] Zhaoming Zhang,[b] Zhiwei Fu,[c*] Jiancheng Zhou[a*]

[a]School of Chemistry and Chemical Engineering, Southeast University, Nanjing 211189, China

[b]Shangdong Yellow Triangle Biotechnology Industry Research Institute Co. Ltd., Dongying 257091, China

[c] Xuzhou B&C Chemical Co. Ltd, Xuzhou 221300, China

[*]Corresponding authors: Naixu Li, E-mail: naixuli@seu.edu.cn;

Zhiwei Fu, E-mail: david@bcpharma.com;

Jiancheng Zhou, E-mail: jczhou@seu.edu.cn

AQE results for 0.10SCCN

The apparent quantum efficiency (AQE) for 0.10SCCN was measured under the same photocatalytic reaction condition except that a 300W Xe lamp supplied the incident light with specific band-pass filters to get the desired incident wavelength (420 nm) light, respectively. The catalyst was irradiated for 4 h. The AQE was calculated by using the equation:

$$\text{AQE (\%)} = \frac{\text{number of reacted electrons } (N_{RE})}{\text{number of absorbed photons} (N_{AP})} \times 100\%, \quad (1)$$

$$N_{RE} \text{ (mol)} = 2 \times \text{yield of } H_2, \quad (2)$$

$$N_{AP} \text{ (mol)} = \frac{\text{absorbed photon flux} \times \text{incident light area} \times \text{radiation time}}{\text{average photo energy} \times N_A}, \quad (3)$$

where absorbed photon flux was 100 mW cm^{-2}, the incident light area was 9.80 cm^2, the radiation time was 14400 s. Average photon energy was $\frac{hc}{\lambda}$ = (6. 62×10^{-34}) × (3×10^{8})/(4.2×10^{-7}) J = 4.73×10^{-19} J.

***λ* = 420 nm:**

$$\textbf{AQE} = \frac{(2 \times 4\text{h} \times 4868\times50\times10^{-3}) \times 10^{-6} \text{ mol}}{(\frac{100 \times 10^{-3}\text{W cm}^{-2} \times 9.8 \text{ cm}^2 \times 14400 \text{ s}}{4.73 \times 10^{-19} \text{ J} \times 6.02 \times 10^{23}})} \times 100\% = 3.93\%$$

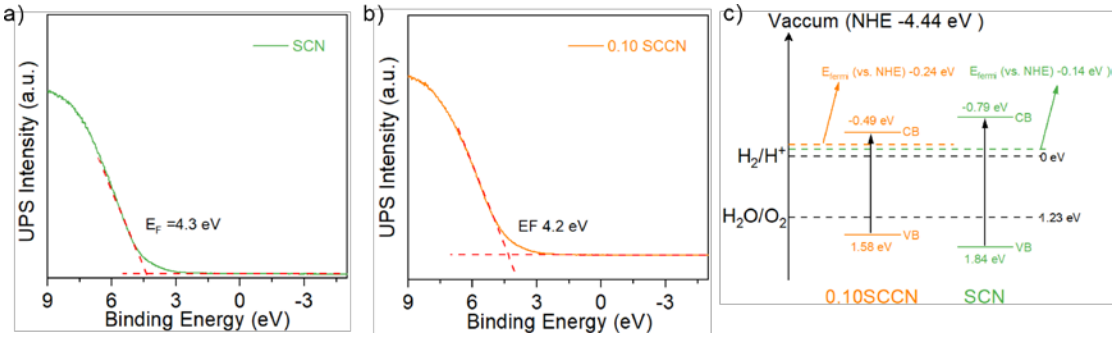

Fig. S1. a) Ultraviolet photoelectron spectroscopy spectrum of SCN and b) 0.10SCCN, c) Schematic band structure of SCN and 0.10 SCCN.

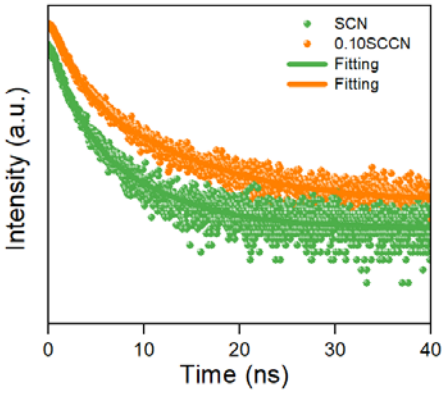

Fig. S2. Time-resolved photoluminescence spectra of SCN and 0.10SCCN.

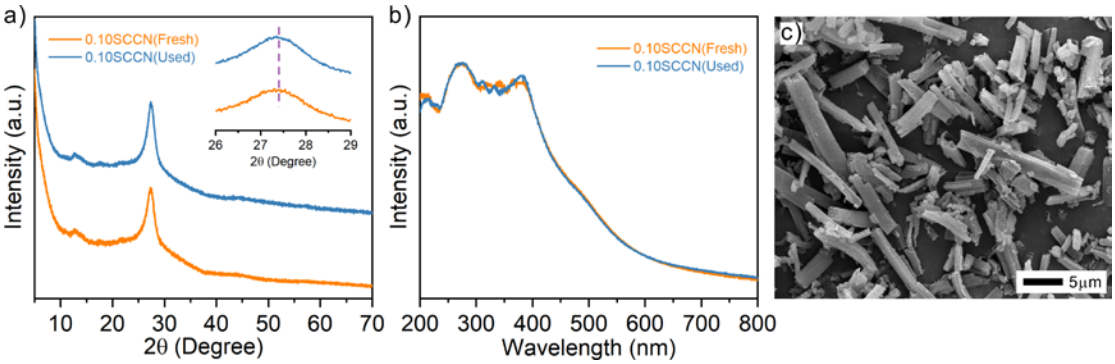

Fig. S3. a) XRD pattern and b) UV-vis diffuse reflection spectra of 0.10SCCN photocatalyst before and after the photocatalytic reaction, c) SEM image of 0.10SCCN after photocatalytic reaction

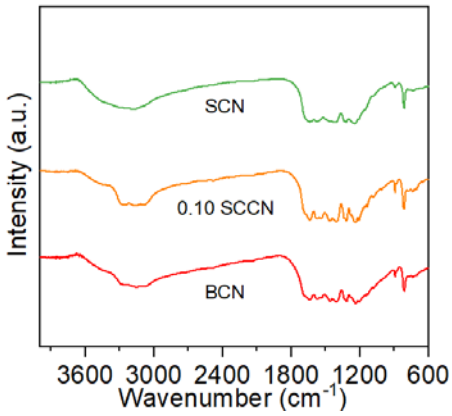

Fig. S4. FTIR spectra of BCN, SCN and SCCN photocatalysts.

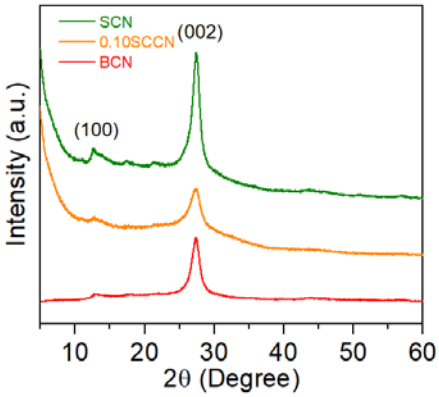

Fig. S5. XRD patterns of BCN, SCN and 0.10SCCN photocatalysts.

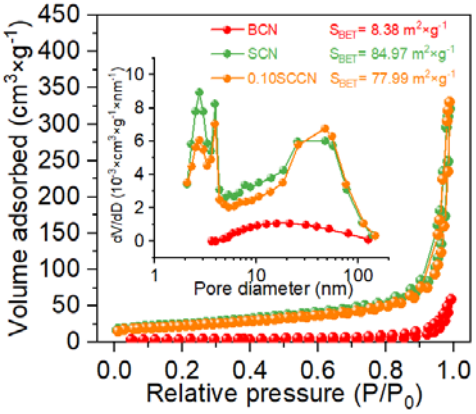

Fig. S6. Nitrogen adsorption-desorption isotherm and the corresponding pore-size distribution curves (inset) of BCN, SCN and 0.10SCCN.

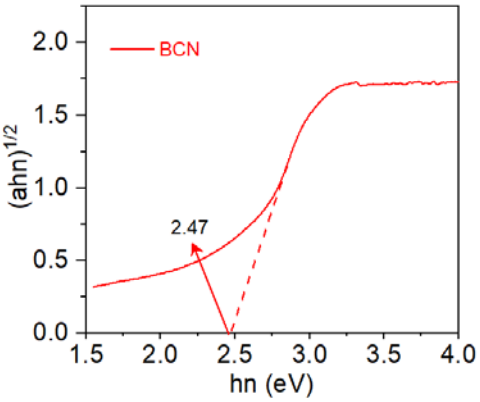

Fig. S7. The bandgap energy of BCN calculated based on Tauc method.

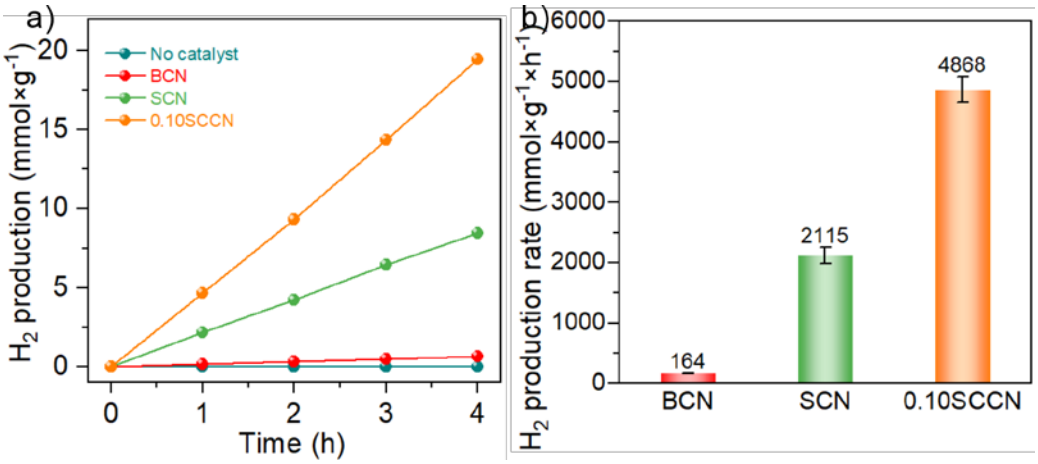

Fig. S8. a) Time course of photocatalytic H_2 production and b) the average H_2 production rate of BCN, SCN and 0.10SCCN photocatalysts.

Table S1 TRPL parameters for photocatalysts.

Sample	τ1 (ns)	A1	τ2 (ns)	A2	Average τ (ns)
SCN	1.55	526.70	5.98	88.24	3.29
0.10SCCN	1.82	826.93	7.70	202.02	4.81

Table S2 Comparison of photocatalytic H_2 production performance of deficient carbon nitride reported in literature

Photocatalyst	Light source	Sacrifice agent	Pt loading/ Dosage (mg)	H_2 production rate ($\mu mol \cdot g^{-1} \cdot h^{-1}$)/the ratio to bulk carbon nitride	Ref (Year)
0.10SCCN	300 W Xe lamp (λ > 420 nm)	TEOA (10 vol%)	3.0 wt%/10	4868/29.6times	This work
Co_2/La_1-g-C_3N_4	300 W Xe lamp (λ > 420 nm)	TEOA (10 vol%)	/	250/2.5 times	[1] (2021)
3Ru/CNHNS	350 W Xe lamp (λ > 420 nm)	methanol-water (5 vol%)	/	3160/15 times	[2] (2021)
RuxP/PCN	350 W Xe lamp (λ > 420 nm)	TEOA (10 vol%)	/	1940	[3] (2021)
NMS/SCN	350 W Xe lamp (λ > 420 nm)	TEOA (10 vol%)	/	658.6	[4] (2021)
Ce6@pCN	300 W Xe lamp (λ > 420 nm)	TEOA (20vol%)	3.0 wt%/10	1527.6/10 times	[5] (2020)
$CNA_{0.2}$	300 W Xe lamp (λ > 420 nm)	TEOA (20 vol%)	3.0 wt%/10	1840.38/6.06 times	[6] (2020)
MoS_2/g-C_3N_4	300 W Xe lamp (λ > 420 nm)	TEOA (0.10M)	3.0 wt%/50	1115/5 times	[7] (2019)
CN-10	300 W Xe lamp (λ > 400 nm)	lactic acid (10 vol%)	3.0 wt%/10	459/5.2 times	[8] (2019)

References

1. Tasleem S, Tahir M. Synergistically improved charge separation in bimetallic Co-La modified 3D g-C_3N_4 for enhanced photocatalytic H_2 production under UV-visible light. International Journal of Hydrogen Energy, 2021, 46 (40): 20995–21012

2. Tahir B, Tahir M, Nawawai M G M, et al. Ru-embedded 3D g-C_3N_4 hollow nanosheets (3D CNHNS) with proficient charge transfer for stimulating photocatalytic H_2 production. International Journal of Hydrogen Energy, 2021, 46 (55): 27997–28010

3. Zhang J G, Zhu Q H, Ma Y F, et al. Photo-generated charges escape from P^+ center through the chemical bridges between P-doped g-C_3N_4 and Ru_xP nanoparticles to enhance the photocatalytic hydrogen evolution. Catalysis Today, 2021, 380: 223–229

4. Chen Y L, Su F Y, Xie H Q, et al. One-step construction of S-scheme heterojunctions of N-doped MoS_2 and S-doped g-C_3N_4 for enhanced photocatalytic hydrogen evolution. Chemical Engineering Journal, 2021, 404: 126498

5. Liu Y F, He M F, Guo R, et al. Ultrastable metal-free near-infrared-driven photocatalysts for H_2 production based on protonated 2D g-C_3N_4 sensitized with Chlorin e6. Applied Catalysis B: Environmental, 2020, 260: 118137

6. Che H N, Li C X, Zhou P J, et al. Band structure engineering and efficient injection rich-π-electrons into ultrathin g-C_3N_4 for boosting photocatalytic H_2-production. Applied Surface Science, 2020, 505: 144564

7. Yuan Y J, Shen Z K, Wu S T, et al. Liquid exfoliation of g-C_3N_4 nanosheets to construct 2D-2D MoS_2/g-C_3N_4 photocatalyst for enhanced photocatalytic H_2 production activity. Applied Catalysis B: Environmental, 2019, 246: 120–128

8. Yang F, Liu D Z, Li Y X, et al. Salt-template-assisted construction of honeycomb-like structured g-C_3N_4 with tunable band structure for enhanced photocatalytic H_2 production. Applied Catalysis B: Environmental, 2019, 240: 64–71